

MHD eigenmodes in a semi-infinite structured solar atmosphere

B. Pintér*, V.M. Čadež, and M. Goossens

Centrum voor Plasma Astrofysica, K.U.Leuven, Celestijnenlaan 200 B, B-3001 Heverlee, Belgium

Received 21 April 1997 / Accepted 22 December 1997

Abstract. Linear eigenmodes are determined for the solar atmosphere in the presence of a gravitational field and a magnetic field. The atmosphere consists of a horizontal nonuniform chromosphere and a semi-infinite nonuniform corona. It is bounded from below by a heavy and immovable photosphere. Inhomogeneity is confined to the vertical direction. The gravitational acceleration is constant and the equilibrium magnetic field is horizontal. The equilibrium temperature increases linearly with height in the chromosphere and is constant in the corona. The equilibrium magnetic field is constant in the chromosphere and it decreases with height in the corona in such a way that the Alfvén speed is constant there.

The results show that there are two sets of eigenmodes which can be viewed as p - and g -modes modified by the immobile lower boundary of the atmosphere and by the magnetic field.

The modes can become damped quasimodes with complex frequencies arising from the resonant coupling of eigenmodes to the local MHD continua in the nonuniform chromospheric layer.

Key words: magnetohydrodynamics (MHD) – methods: numerical – Sun: atmosphere – Sun: oscillations

1. Introduction

A fundamental property of nonuniform magnetic plasmas is that they can support local resonant Alfvén waves and resonant slow waves. In ideal MHD, these resonant waves can exist on individual magnetic surfaces without mutual interaction with those on the neighbouring magnetic surfaces. This extreme localization shows up through the non-square integrable spatial solutions of the ideal MHD equations.

The inclusion of dissipative effects, which are always present in real plasmas, results into an interaction between the neighbouring magnetic surfaces and produces finite spatial solutions at the locations where the ideal MHD solutions diverge.

Send offprint requests to: B. Pintér

* On leave from Eötvös L. University, H-1083 Budapest, Hungary

Since each magnetic surface has its own local Alfvén frequency and its own local slow frequency, a nonuniform magnetic equilibrium has a continuum of resonant Alfvén frequencies and a continuum of resonant slow frequencies. In addition to these continuous parts, the linear spectrum of a magnetic plasma contains discrete eigenmodes.

An interesting situation takes place when the frequency of a discrete eigenmode falls within the Alfvén or the slow continuum. In that case a global eigenmode is in resonance with a continuum wave and this produces a damped mode, known as a quasi mode.

Sakurai et al. (1991a,b) designed a method for treating the divergencies in the ideal MHD equations for a nonuniform plasma in absence of gravity, by considering the comparatively narrow dissipative layers around the locations of the resonances. They obtained jump conditions for the vertical component of the Lagrangian displacement ξ_z and for the total pressure perturbation P , which connect their values between the end points of the dissipative layer. The review article on this subject by Goossens & Ruderman (1995) gives a broad list of related references and details of the method also known as the SGHR procedure. The method, originally derived for the driven problem, was extended by Tirry & Goossens (1996) and Tirry et al. (1997a) to treat the eigenvalue problem in nonuniform plasmas without gravity.

A current interest is to study the coupling of waves originating in the much denser interior of the sun to waves that can eventually be observed in the corona. This coupling is of practical importance for diagnostic purposes and for solar seismology in general and its characteristics were broadly studied by Evans & Roberts (1990), Miles & Roberts (1992), Miles, Allen & Roberts (1992) and Jain & Roberts (1993, 1994). In these papers resonances were excluded by the choice of the wave number and/or the equilibrium model. The paper by Tirry et al. (1997) extends these studies to configurations of the atmosphere that permit resonances. In this case the quasi eigenmodes are obtained and their frequencies are somewhat shifted with respect to those obtained in ideal MHD.

The objective of this paper is to investigate the linear eigenmodes of a nonuniform magnetic stellar atmosphere alone i.e. without coupling to the photospheric modes. For this reason, a solid boundary is taken at the bottom of the atmosphere. Such

an assumption is reasonable as the plasma density of the atmosphere is much lower than the density of the photosphere. To solve the eigenvalue problem numerically, we extended the SGHR method to plasmas that are stratified by gravity and we derive the jump conditions for ξ_z and P . We shall focus our attention on the possible shifts of discrete eigenmodes into both continua that would give quasimodes.

The paper is organized as follows: Sect. 2 contains the description of the equilibrium model. The basic equations and assumptions concerning the linear perturbations are given in Sect. 3 while the solutions of the MHD equations are obtained in Sect. 4. The procedure for solving the eigenproblem for our model atmosphere is described briefly in Sect. 5. Sect. 6 contains the results and the discussion of these results. The final conclusions are given in Sect. 7.

2. The model of a semi-infinite atmosphere

The solar atmosphere can be modeled as a semi-infinite region of plasma that occupies the space above the xy -plane in Cartesian coordinates with the z -axis taken along the gravitational acceleration $\mathbf{g} = -g\mathbf{e}_z$ and $g = \text{const}$.

The magnetic field is horizontal throughout the whole space, i.e. $\mathbf{B}_0 = (B_0, 0, 0)$ while the physical quantities in the basic state (like B_0 , ρ_0 , p_0 and T_0) are taken inhomogeneous in z only. The present model atmosphere is a fully ionized plasma and consists of a chromosphere and a corona. The chromosphere is represented by a layer between $z = 0$ and $z = L_c$ where the plasma temperature T_0 increases linearly with z while the horizontal magnetic field remains uniform $B_0 = \text{const}$. The overlying region, the corona, is of infinite vertical extent, with constant plasma temperature and constant Alfvén speed.

The system is initially in magnetohydrostatic equilibrium:

$$\frac{dp_0}{dz} + \frac{d}{dz} \frac{B_0^2}{2\mu_0} + \rho_0 g = 0. \quad (1)$$

The unperturbed plasma is taken ideal as the dissipative effects can be neglected on the time scale typical for the MHD wave phenomena.

The full model of the atmosphere with the chromosphere and the corona is shown schematically in Fig. 1.

The chromosphere, $L_c \geq z \geq 0$: The layer $L_c \geq z \geq 0$ models the chromosphere in which the temperature profile is a linear function of z :

$$T_0(z) = T_p \left(1 + \frac{z}{L}\right) \quad (2)$$

The characteristic length L in (2) is expressed in terms of the ratio of the coronal to the photospheric temperature $\tau \equiv T_0(L_c)/T_0(0) \equiv T_c/T_{ph}$ and is given by:

$$L = \frac{L_c}{\tau - 1}. \quad (3)$$

The assumption of $B_0 = \text{const}$ simplifies the Eq. (1) for the equilibrium state in the chromosphere to

$$\frac{dp_0}{dz} + \rho_0 g = 0, \quad (4)$$

where

$$p_0 = \rho_0 \mathcal{R} T_0, \quad (5)$$

according to the perfect gas law. Here $\mathcal{R} \equiv \mathcal{R}_0/\tilde{\mu}$ is the gas constant for a fully ionized hydrogen plasma of the atmosphere, $\tilde{\mu} = 0.6$ is the related mean molar mass and $\mathcal{R}_0 = 8.317 \text{ J kg}^{-1} \text{ K}^{-1}$ is the universal gas constant.

The temperature profile (2), together with the equation of magnetostatics (4) and the perfect gas law (5), yield the following distributions for the unperturbed pressure p_0 and density ρ_0 :

$$p_0(z) = \frac{p_p}{(1+z/L)^{L/H}}, \quad \rho_0(z) = \frac{\rho_p}{(1+z/L)^{1+L/H}}. \quad (6)$$

Here $H = \mathcal{R} T_p / g$ is the photospheric isothermal scale height, while T_p , p_p and ρ_p are the photospheric values of temperature, gas pressure and density respectively taken at $z = 0$.

In the analysis of linear motions, the speed of sound v_s , the Alfvén speed v_A and the cusp speed v_c will play an important role. They are defined as

$$v_s^2(z) \equiv \gamma \mathcal{R} T_0(z),$$

$$v_A^2(z) \equiv \frac{B_0^2}{\mu_0 \rho_0(z)} = \frac{2}{\gamma \beta(z)} v_s^2(z) \quad (7)$$

$$v_c^2(z) = \frac{v_A^2(z) v_s^2(z)}{v_A^2(z) + v_s^2(z)} = \frac{2}{2 + \gamma \beta(z)} v_s^2(z),$$

where γ is the ratio of specific heats and $\beta \equiv p_0/p_m = 2v_s^2/\gamma v_A^2$ is the ratio of gas pressure p_0 to plasma pressure $p_m \equiv B_0^2/(2\mu_0)$. In the present model β depends on z as

$$\beta(z) = \beta_p \left(1 + \frac{z}{L}\right)^{-L/H} \quad (8)$$

so that the expressions (7) become

$$v_s^2(z) = v_{sp}^2 \left(1 + \frac{z}{L}\right), \quad v_A^2(z) = \frac{2}{\gamma \beta_p} v_{sp}^2 \left(1 + \frac{z}{L}\right)^{1+L/H},$$

$$v_c^2(z) = 2v_{sp}^2 \frac{\left(1 + \frac{z}{L}\right)^{L/H}}{2 \left(1 + \frac{z}{L}\right)^{L/H} + \gamma \beta_p}. \quad (9)$$

The corona, $z > L_c$: Above the chromospheric layer, both v_s^2 and v_A^2 are assumed continuous across the boundary $z = L_c$ and constant at $z > L_c$:

$$v_s^2(z) = \tau v_{sp}^2 = \text{const}, \quad (10)$$

$$v_A^2(z) = \frac{2\tau^{1+L/H}}{\gamma \beta_p} v_{sp}^2 = \text{const}.$$

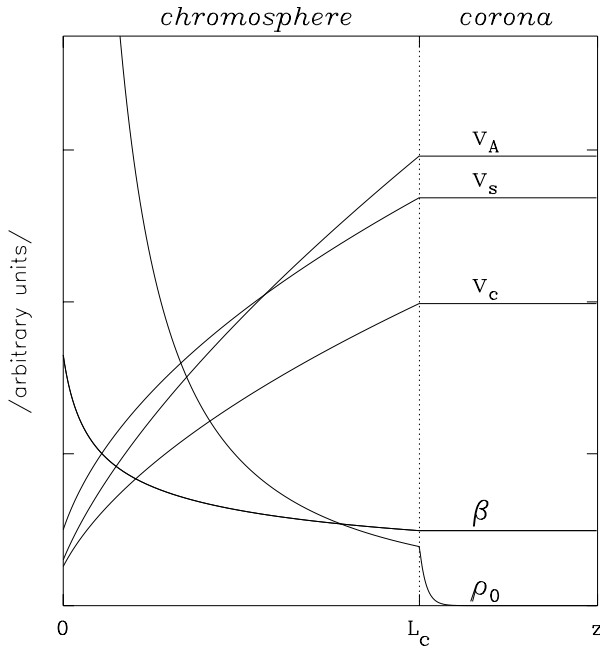


Fig. 1. A schematic model of the considered atmosphere showing the profiles of the relevant parameters. The indicated quantities are given in arbitrary units.

Consequently, the plasma parameter β is constant in the corona with its value β_c , related to the photospheric value β_p as:

$$\beta_c = \tau^{-L/H} \beta_p. \quad (11)$$

The magnetohydrostatic equation (1) can then be written as

$$\left(\frac{v_s^2}{\gamma} + \frac{v_A^2}{2} \right) \frac{d\rho_0}{dz} + \rho_0 g = 0,$$

and solved for the density distribution $\rho_0(z)$:

$$\rho_0 = \rho_{0c} e^{(L_c - z)/I}, \quad (12)$$

where

$$\rho_{0c} = \rho_p \tau^{-(1+L/H)} \quad \text{and} \quad I = \frac{1 + \beta_c}{\beta_c} \tau H.$$

with β_c given by (11).

3. Basic equations and assumptions

We use the linearized version of the MHD equations for studying the linear eigenoscillations of the solar atmosphere.

As explained in the introduction, the main goal of the present paper is to study quasimodes in the linear spectrum. Quasimodes are damped eigenmodes and need to be treated, in principle, by dissipative MHD. In the present paper, we include Ohmic heating as the only dissipative effect in the MHD equations.

Other dissipative effects, such as viscosity and thermal conductivity, are found less important in typical stellar atmospheres (Goossens, Ruderman & Hollweg, 1995).

The standard set of linearized equations of resistive MHD is then:

$$\begin{aligned} \frac{\partial \rho_1}{\partial t} + \nabla \cdot (\rho_0 \mathbf{v}_1) &= 0, \\ \rho_0 \frac{\partial \mathbf{v}_1}{\partial t} &= -\nabla p_1 + \frac{1}{\mu_0} (\nabla \times \mathbf{B}_1) \times \mathbf{B}_0 \\ &\quad + \frac{1}{\mu_0} (\nabla \times \mathbf{B}_0) \times \mathbf{B}_1 + \rho_1 \mathbf{g}, \end{aligned} \quad (13)$$

$$\frac{\partial \mathbf{B}_1}{\partial t} = \nabla \times (\mathbf{v}_1 \times \mathbf{B}_0) + \eta \nabla^2 \mathbf{B}_1,$$

$$\frac{\partial p_1}{\partial t} + \mathbf{v}_1 \cdot \nabla p_0 = v_s^2 \left(\frac{\partial \rho_1}{\partial t} + \mathbf{v}_1 \cdot \nabla \rho_0 \right).$$

Since the equilibrium quantities depend on the spatial coordinate z only, the perturbed quantities are Fourier analyzed with respect to the ignorable spatial coordinates x and y and put proportional to $\exp(ik_x x + ik_y y)$ with k_x and k_y the components of the horizontal wave vector. In a normal mode analysis the time dependence is prescribed by the factor $\exp(-i\omega t)$ where ω is the eigenfrequency that has to be determined. The perturbed quantities then take the form:

$$f_1(x, y, z, t) = f(z; \omega, k_x, k_y) e^{i(k_x x + k_y y - \omega t)}.$$

The magnetic Reynolds number has very large values under conditions found in the solar and stellar atmospheres. This implies that dissipation due to finite electrical conductivity can be ignored with exceptions of localized domains where steep gradients occur. In these dissipative regions, the Eqs. (13) of resistive MHD are required for a physically meaningful description of MHD waves while ideal MHD gives an accurate description of the wave dynamics elsewhere.

In the region where the approximation of ideal MHD is applicable, the set of linearized ideal MHD equations (13) with $\eta = 0$, reduces to two ordinary differential equations of the first order for the vertical component of the Lagrangian displacement ξ_z ($\equiv -i\omega v_z$) and for the Eulerian perturbation of total (magnetic and thermal) pressure perturbation P :

$$D \frac{d\xi_z}{dz} = C_1 \xi_z - C_2 P, \quad D \frac{dP}{dz} = C_3 \xi_z - C_1 P. \quad (14)$$

The coefficient functions D , C_1 , C_2 and C_3 are

$$\begin{aligned} D &= \rho_0 (v_s^2 + v_A^2) (\omega^2 - \omega_c^2) (\omega^2 - \omega_A^2), \\ C_1 &= g \rho_0 \omega^2 (\omega^2 - \omega_A^2), \\ C_2 &= (\omega^2 - \omega_A^2) (\omega^2 - \omega_s^2) - \omega^2 v_A^2 k_y^2, \\ C_3 &= \left[\rho_0 (\omega^2 - \omega_A^2) + g \frac{d\rho_0}{dz} \right] D + g^2 \rho_0^2 (\omega^2 - \omega_A^2)^2 \end{aligned} \quad (15)$$

Here ω_s , ω_A and ω_c are the local sound frequency, the local Alfvén frequency and the local cusp frequency. Their squares are given by

$$\omega_s^2 = v_s^2(k_x^2 + k_y^2), \quad \omega_A^2 = v_A^2 k_x^2, \quad \omega_c^2 = v_c^2 k_x^2.$$

Eqs. (14) govern the linear motions of a one-dimensional magnetic plasma in a gravitational field. When these equations are supplemented with boundary conditions they define an eigenvalue problem for ω .

These boundary conditions are $\xi_z(0) = 0$ at the lower boundary ($z = 0$) and the continuity of both $P(z)$ and $\xi_z(z)$ at the upper boundary ($z = L_c$). In addition, we require that the kinetic energy of perturbation $\frac{1}{2}\rho_0(z)\omega|\xi(z)|^2$ vanishes as $z \rightarrow \infty$. This condition means that we restrict the analysis to non-leaky eigenmodes whose energy remains practically localized to a finite region above the photosphere. The solution is normalized by imposing $P(0) \equiv 1$.

The ordinary differential equations (14) of ideal MHD are singular at locations $z = z_A$ and $z = z_c$ where the coefficient function D vanishes, i.e. when either of the two conditions

$$\omega = \omega_A(z_A) \quad \text{or} \quad \omega = \omega_c(z_c) \quad (16)$$

for the Alfvén resonance or the cusp resonance is satisfied.

The frequency matching (16) indicates the existence of a resonant wave transformation due to the excitation of a local Alfvén MHD at $z = z_A$ mode or a slow mode at $z = z_c$.

Because of the singularities in Eqs. (14), the solutions and their z -derivatives diverge at the resonant points z_c and z_A . Thus, the ideal MHD equations (14) fail to give physically acceptable results within a comparatively thin layer around the position where the resonant condition (16) is satisfied. Consequently, dissipation has to be included and the resistive MHD equations (13) are to be applied there.

The dissipation makes the eigenmodes damped and the related eigenfrequency becomes complex: $\omega = \omega_r + i\omega_i$ where $|\omega_r| \gg |\omega_i|$. In this case, the resonances occur when the real part of the eigenfrequency satisfies the conditions (16):

$$\omega_r = \omega_A(z_A) \quad \text{or} \quad \omega_r = \omega_c(z_c). \quad (17)$$

4. Solutions of MHD equations

4.1. The corona: $z \geq L_c$

Solutions to Eqs. (14) can be obtained in a closed analytic form for an equilibrium model with constant v_s and v_A . In this case, the Eqs. (14) can be written as

$$\frac{d\zeta}{dz} = \left(A_1 - \frac{1}{I}\right)\zeta - A_2 P \quad (18)$$

$$\frac{dP}{dz} = A_3 \zeta - A_1 P$$

where $\zeta \equiv \rho_0(z)\xi_z(z)$ and the density $\rho_0(z)$ is given by Eq. (12). Quantities $A_1 \equiv C_1(z)/D(z)$, $A_2 \equiv C_2\rho_0(z)/D(z)$ and $A_3 \equiv C_3(z)/(\rho_0(z)D(z))$ are now constant coefficients:

$$A_1 = \frac{g\omega^2}{(v_s^2 + v_A^2)(\omega^2 - \omega_c^2)}$$

$$A_2 = \frac{(\omega^2 - \omega_A^2)(\omega^2 - \omega_s^2) - \omega^2 v_A^2 k_y^2}{(v_s^2 + v_A^2)(\omega^2 - \omega_A^2)(\omega^2 - \omega_c^2)}$$

$$A_3 = \frac{(v_s^2 + v_A^2)(\omega^2 - \omega_c^2) \left(\omega^2 - \omega_A^2 - \frac{g}{I}\right) + g^2(\omega^2 - \omega_A^2)}{(v_s^2 + v_A^2)(\omega^2 - \omega_c^2)}$$

with constant speeds v_A and v_s given by Eqs. (10). These constant coefficients are:

The general solution of Eqs. (18) is now immediately obtained as:

$$\xi_z = a_1 e^{-K^{(-)}(z-L_c)} + a_2 e^{K^{(+)}(z-L_c)},$$

$$P = (A_1 + K^{(-)})\frac{\rho_{0c}}{A_2} a_1 e^{-K^{(+)}(z-L_c)} \quad (19)$$

$$+(A_1 - K^{(+)})\frac{\rho_{0c}}{A_2} a_2 e^{K^{(-)}(z-L_c)}.$$

$a_{1,2}$ are integration constants, $\rho_{0c} = \tau^{1+L/H}$ according to Eq. (12), and

$$K^{(\pm)} = \kappa \pm \frac{1}{2I} \quad \text{with} \quad \kappa^2 = \left(A_1 - \frac{1}{2I}\right)^2 - A_2 A_3, \quad (20)$$

or

$$\kappa^2 = -\frac{(\omega^2 - \omega_I^2)(\omega^2 - \omega_{II}^2)(\omega^2 - \omega_{III}^2)}{(v_s^2 + v_A^2)(\omega^2 - \omega_A^2)(\omega^2 - \omega_c^2)}. \quad (21)$$

The frequencies $\omega_{I,II,III}$ play the role of cut-off frequencies and are solutions to the equation

$$\omega^6 + \mathcal{H}_4 \omega^4 + \mathcal{H}_2 \omega^2 + \mathcal{H}_0 = 0$$

where

$$\mathcal{H}_0 = g^2 k^2 \omega_A^2 - \left(\frac{1}{4I^2} + k^2\right) \omega_A^4 v_s^2 - \frac{g}{I} \omega_A^2 v_s^2 k^2,$$

$$\mathcal{H}_2 = \left(\frac{1}{4I^2} + k^2\right) (v_s^2 + 2v_A^2) \omega_A^2$$

$$+ \frac{g}{I} [(v_s^2 + v_A^2)k^2 - \omega_A^2] - g^2 k^2,$$

$$\mathcal{H}_4 = -\left(\frac{1}{4I^2} + k^2\right) (v_s^2 + v_A^2) - \omega_A^2.$$

The coefficient κ^2 depends on the eigenfrequency and can be a complex number. For discrete eigenmodes outside the Alfvén and the slow continua, the eigenvalue ω is purely real and so is κ^2 . For discrete eigenmodes within the Alfvén continuum and/or the slow continuum the eigenvalue ω and the quantity κ^2 are complex with $|\text{Im } \omega| \ll |\text{Re } \omega|$.

The necessary existence conditions for eigenmodes are thus

$$a_2 = 0 \quad \text{and} \quad \kappa^2 > 0 \quad \text{if} \quad \text{Im } \kappa^2 = 0. \quad (22)$$

4.2. The chromosphere: $L_c \geq z \geq 0$

The solutions to Eqs. (14) that govern the linear eigenmodes in ideal MHD, cannot be obtained in a closed analytic form in the chromosphere. The profiles of the basic state quantities given by (6) and (9) require now a numerical integration in the layer $L_c \geq z \geq 0$.

Since $v_s^2(z)$ and $v_A^2(z)$ vary with z , the resonant conditions might be satisfied here. If this is indeed the case, ideal MHD produces divergent solutions in the resonant points z_A or/and z_c . In the vicinity of these singular points, dissipation is important and it has to be taken into account in the analysis of eigenmodes. For this reason, we derive from (13) an approximative set of dissipative equations valid in an interval which encloses the dissipative layer containing the singularity.

This analysis follows Sakurai et al. (1991a,b) and Goossens et al. (1995), commonly applied to various nonuniform plasma configurations in absence of gravitational effects.

As to the eigenmode analysis, it suffices to know how to connect the ideal solutions over the dissipative layer. These connection formulae for a nonuniform plasma in the presence of a gravitational field are derived below along the lines of the analysis by Goossens et al. (1995).

The cusp resonance: In the region close to the cusp resonance we have $\omega_r \approx \omega_c$ according to (17), and the eigenfrequency can be taken as $\omega \approx \omega_c + i\omega_i$. The small imaginary part ω_i comes from dissipation and it is responsible for wave damping.

The resistive MHD equations (13) can now be reduced to the following approximative set of two third order differential equations:

$$\begin{aligned} & \left[s\Delta_c + i\omega_c \left(2\omega_i - \eta \frac{d^2}{ds^2} \right) \right] \frac{d\xi_z}{ds} \\ &= \frac{k_x^2 v_s^4}{\rho_0 (v_s^2 + v_A^2)^2} \left(g\rho_0 \frac{v_A^2}{v_s^2} \xi_z + P \right), \\ & \left[s\Delta_c + i\omega_c \left(2\omega_i - \eta \frac{d^2}{ds^2} \right) \right] \frac{dP}{ds} \\ &= -g \frac{k_x^2 v_s^2 v_A^2}{(v_s^2 + v_A^2)^2} \left(g\rho_0 \frac{v_A^2}{v_s^2} \xi_z + P \right). \end{aligned} \quad (23)$$

The new variable $s \equiv z - z_c$ is the distance from the cusp resonant point, $\Delta_c \equiv d(\omega^2 - \omega_c^2)/ds$ and all coefficients in (23) are constant and have their values taken at $s = 0$.

The half-width δ_c of the dissipative layer and the rate of wave damping ω_i are estimated from assumptions that all three terms on the left-hand side of Eqs. (23) are of the same order of magnitude:

$$|s\Delta_c| \sim |2\omega_c\omega_i| \sim \left| \eta\omega_c \frac{d^2}{ds^2} \right|$$

Dissipation is important when the ideal term $|s\Delta_c|$ and the non-ideal terms $\left| \eta\omega_c \frac{d^2}{ds^2} \right|$ and $|2\omega_c\omega_i|$ in the left-hand side of Eq. (23) are comparable. This leads to:

$$\delta_c = \left(\frac{\eta\omega_c}{|\Delta_c|} \right)^{1/3} \quad \text{and} \quad |\omega_i| \sim \frac{1}{2} \eta^{1/3} \left(\frac{|\Delta_c|}{\omega_c} \right)^{2/3}, \quad (24)$$

where δ_c is a measure for the thickness of the dissipative layer.

The solutions to Eqs. (14) can be expressed in terms of the \tilde{F} and \tilde{G} functions of Ruderman et al. (1995) and Tirry & Goossens (1996). The results by Tirry & Goossens (1996) show that the differences between the dissipative and the ideal solutions are negligible for $|s| \geq 5\delta_c$.

Multiplying the first equation in (23) by gv_s^2 , the second one by v_s^2/ρ_0 and then adding them up, we obtain the conservation law

$$C_c \equiv g\rho_0 \frac{v_A^2}{v_s^2} \xi_z + P = \text{const.} \quad (25)$$

The important consequence of (25) is that we can get the amplitude differences or jumps between $z = z_c \pm 5\delta_c$ for both the Lagrangian displacement ξ_z and the total pressure perturbation P :

$$\begin{aligned} [\xi_z]_c &= -i\pi k_x^2 \frac{v_s^4}{|\Delta_c| \rho_0 (v_s^2 + v_A^2)^2} C_c, \\ [P]_c &= i\pi g k_x^2 \frac{v_s^2 v_A^2}{|\Delta_c| (v_s^2 + v_A^2)^2} C_c. \end{aligned} \quad (26)$$

We see from Eqs. (26) that the jump conditions are independent of the specific type of dissipation and that P is not constant across the dissipative layer when gravity is present.

The Alfvén resonance: A completely analogous analysis is carried out for the Alfvén resonance at $z = z_A$.

The third order differential equations for ξ_z and P close to z_A are here:

$$\begin{aligned} & \left[s\Delta_A + i\omega_A \left(2\omega_i - \eta \frac{d^2}{ds^2} \right) \right] \frac{d\xi_z}{ds} = \frac{k_y^2}{\rho_0} P, \\ & \left[s\Delta_A + i\omega_A \left(2\omega_i - \eta \frac{d^2}{ds^2} \right) \right] \frac{dP}{ds} = 0, \end{aligned} \quad (27)$$

where $s \equiv z - z_A$, $\Delta_A \equiv d(\omega^2 - \omega_A^2)/ds$ and all quantities have their values taken at $z = z_A$.

The second equation in (27) indicates the constancy of the Eulerian perturbation of total pressure across the domain around the Alfvén resonance point:

$$C_A = P = \text{const.}$$

Finally, the jump conditions between $z = z_A \pm 5\delta_A$ are:

$$[\xi_z]_A = -i\pi \frac{k_y^2}{|\Delta_A| \rho_0} P, \quad [P]_A = 0. \quad (28)$$

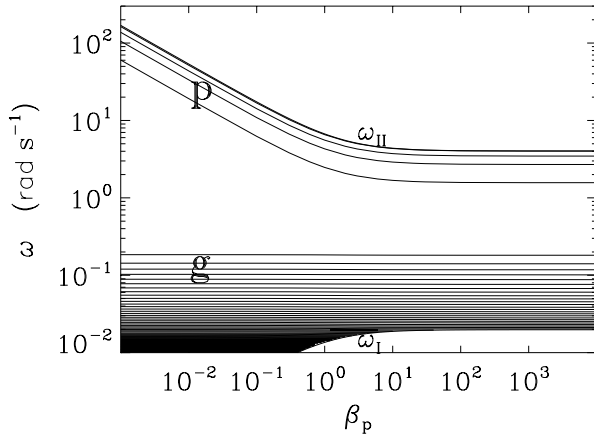


Fig. 2. The frequencies of modified p - and g -modes with $k_x=0$ and $k_y=3.6 \text{ Mm}^{-1}$ plotted as a function of β_p

and δ_A is again taken from Tirry & Goossens (1996) as

$$\delta_A \approx \left(\frac{\eta \omega_A}{|\Delta_A|} \right)^{1/3}. \quad (29)$$

Here also, as for the slow-resonance dissipation does not show up explicitly in the jump conditions.

5. Eigenvalue solutions

Eqs. (14) supplemented with the boundary conditions defines the eigenvalue problem for the linear motions of the model atmosphere specified in Sect. 2.

For each set of wavenumbers k_x and k_y there is a spectrum of eigenmodes. Hence we first have to set the values of the wavenumbers k_x and k_y and subsequently we try and compute the spectrum (or part of the spectrum). This is done by the method of trial and error. We choose a trial value for ω and integrate the ideal Eqs. (14) numerically by a Runge Kutta method. This numerical integration starts from $z = 0$ taking $\xi_z(0) = 0$ and normalizing the solution by choosing $P(0) = 1$. If the resonant condition $\omega = \omega_{A,c}(z)$ is satisfied at $z = z_{A,c}$ for a given ω , which is checked before the numerical integration is carried out, the corresponding dissipative layer is left out of the integration scheme and crossed by use of connection formulae at $z_A \pm 5\delta_A$. The numerical integration ends at the upper boundary $z = L_c$ where the resulted numerical values for $\xi_z(L_c) \equiv \xi_{zc}$ and $P(L_c) \equiv P_c$ have to be matched to the values (19) obtained analytically in the region $z \geq L_c$. This then yields the following expressions for amplitudes a_1 and a_2 in (19):

$$\begin{aligned} a_1 &= \frac{A_2 P_c + (K^{(+)} - A_1) \rho_{0c} \xi_{zc}}{2 \rho_{0c} \kappa} \\ a_2 &= \frac{(K^{(-)} + A_1) \rho_{0c} \xi_{zc} - A_2 P_c}{2 \rho_{0c} \kappa} \end{aligned} \quad (30)$$

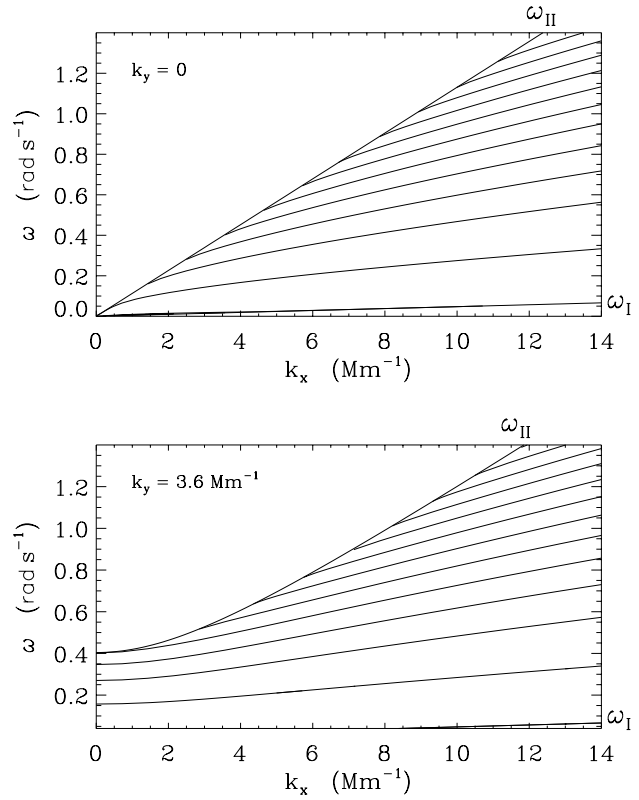


Fig. 3. The spectrum of modified p -modes at $\beta_p=1,000$ for $k_y=0$ and $k_y=3.6 \text{ Mm}^{-1}$. The eigenmodes exist between the cut-off frequencies ω_I and ω_{II} .

The necessary existence conditions (22) for eigenmodes now become:

$$(K^{(-)} + A_1) \rho_{0c} \xi_{zc} - A_2 P_c = 0 \quad (31)$$

$$\kappa^2 > 0 \text{ if } \mathcal{I}m \kappa^2 = 0$$

with values for v_A^2 , v_s^2 and ρ_0 taken at $z = L_c + 0$.

Finally, only those perturbations that satisfy the conditions (31) are the eigenmodes that remain localized inside the atmosphere. The waves that are not eigenmodes will either disappear from the atmosphere as leaky waves or will require an infinite energy at finite initial perturbation amplitudes.

6. Numerical results

For solving the eigenmode equations we need to specify the equilibrium density ρ_0 and characteristic speeds v_s , v_A , v_c . This is done by prescribing numerical values for g , v_{sp} , L , H , and β_p in Eqs. (6) and (9).

Numerical calculations were performed for values that are related to the solar atmosphere. Thus the gravitational acceleration at $z=0$ is $g=g_\odot=274 \text{ m s}^{-2}$, the photospheric speed of sound is $v_{sp}=8 \text{ km s}^{-1}$ corresponding to the photospheric temperature $T_{ph}=6,000 \text{ K}$ and the isothermal pressure scale height H is $H \approx 140 \text{ km}$. The location of the upper boundary of the

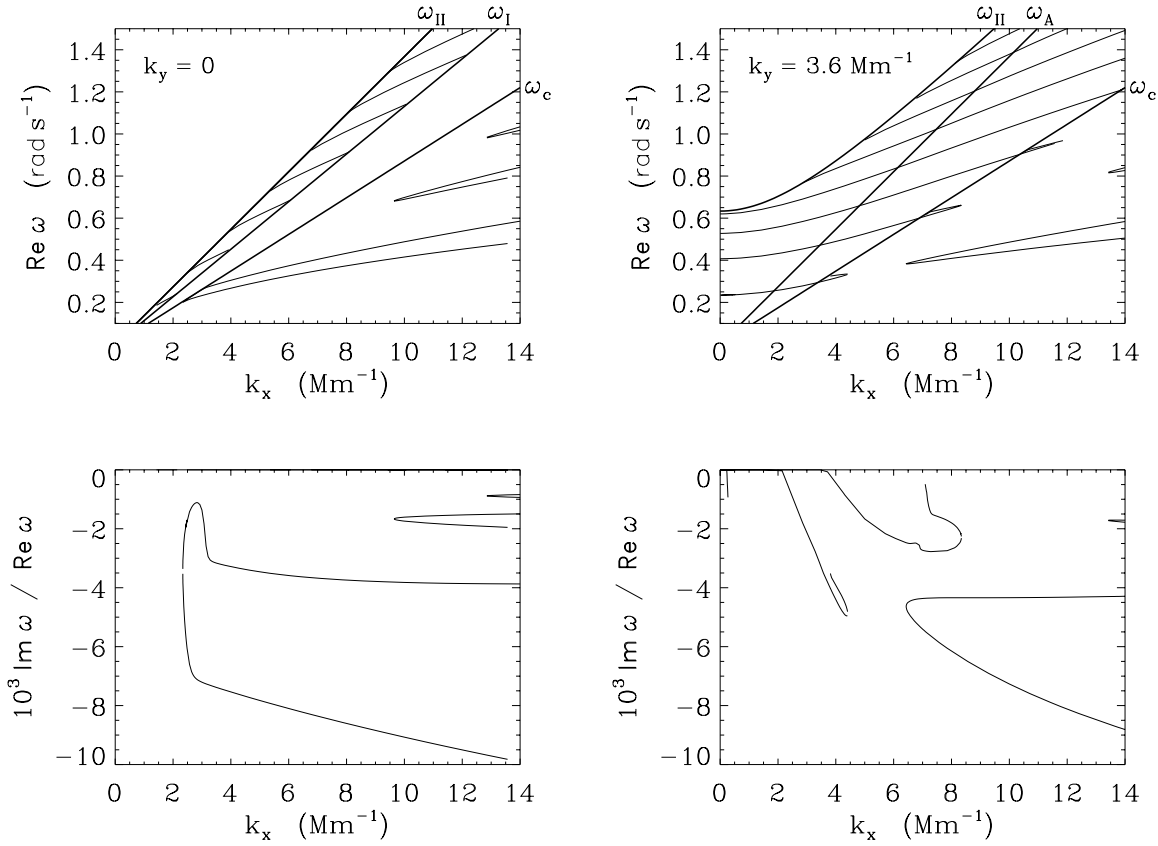


Fig. 4. The spectrum of modified p -modes for $k_y=0$ and $k_y=3.6 \text{ Mm}^{-1}$; $\beta_p=1.2$. Complex frequencies correspond to quasimodes that are resonantly coupled to local Alfvén and/or cusp continua. Characteristic frequencies ω_I , ω_{II} , ω_A and ω_c refer to the values in the corona, at $z \geq L_c$.

inhomogeneous region is taken at $z=L_c=2 \text{ Mm}$, the temperature variation length is then $L=L_c/(\tau-1)$ and the related temperature gradient in the chromospheric layer is $dT_0/dz=T_{ph}/L$. The temperature ratio $\tau \equiv T_c/T_{ph}$ is chosen to be $\tau=200$.

We have taken two values for plasma beta at the photospheric level $z=0$. The first value is $\beta_p=1,000$ and corresponds to a weak magnetic field (the atmosphere is practically nonmagnetic). The second value is $\beta_p=1.2$ so that $v_{sp}=v_{Ap}$ i.e. that the speed of sound and the Alfvén speed are equal at $z=0$ and corresponds to a relatively strong magnetic field.

The eigenspectrum is then calculated numerically from Eq. (31). The frequencies are complex if at least one of the two resonances occurs in the transition layer below the uniform corona. A negative imaginary part of the frequency means that the eigenmodes are damped by resonant coupling to local continuum oscillations.

Before we proceed to discuss our results, it is instructive to point out that the spectrum of a nonmagnetic atmosphere consists of an infinite Sturmian sequence of acoustic eigenmodes with a clusterpoint at $+\infty$ and an infinite anti-Sturmian sequence of gravity eigenmodes with a clusterpoint at $\omega=0$.

The anti-Sturmian gravity sequence is stable if the square of the buoyancy frequency $N^2=-g(\frac{1}{\rho} \frac{d\rho}{dz} - \frac{1}{\gamma p} \frac{dp}{dz})$ is positive everywhere.

Let us now look at motions with $k_x=0$. For these motions the local Alfvén frequency and the local cusp frequency are identically zero and the only effect of the magnetic field is to provide an extra pressure so that v_s^2 is replaced with $v_s^2+v_A^2$. The spectrum for $k_x=0$ is shown in Fig. 2 as a function of β . This figure clearly shows that the spectrum consists of two well separated parts: a high frequency subspectrum of fast acoustic eigenmodes or p -modes and a low frequency subspectrum of gravity eigenmodes.

The fast subspectrum is Sturmian in the sense that the number of nodes in the eigensolution ξ_z increases with increasing eigenfrequency. The fast subspectrum is bounded from above by $\omega_{II} \equiv \omega(L_c)$ and contains a finite number of eigenmodes.

The slow subspectrum (gravity modes) is anti-Sturmian and it is relatively insensitive to variation of β when $k_x=0$. Gravity modes of low and intermediate radial order are totally unaffected by variation of β . Gravity modes of high radial order feel the variation of β essentially because the lower cut-off frequency ω_I increases when β is increased. The effect of a variation of β on the subspectrum of p -modes is more pronounced. An increase in β produces a corresponding decrease in the eigenfrequencies of p -modes up to a point where eigenfrequencies become practically constant with respect to β .

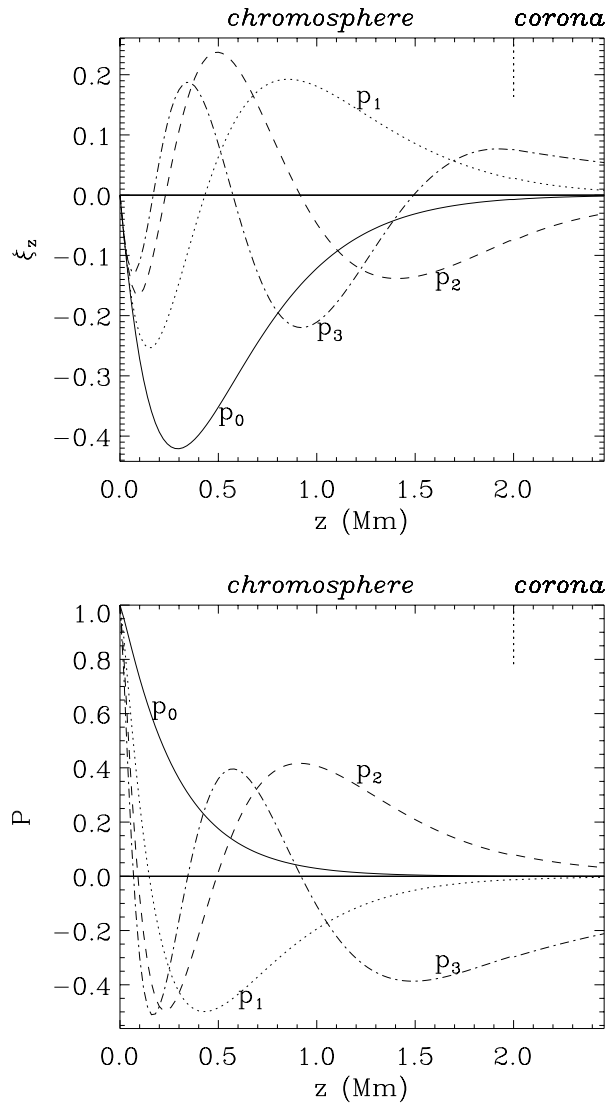


Fig. 5. The eigensolutions of ξ_z and P for p -modes with $k_y=3.6 \text{ Mm}^{-1}$ and $k_x=0.07 \text{ Mm}^{-1}$ at $\beta_p=1.2$. The solutions show that the number of nodes grows with the eigenfrequency indicating the Sturmian character of the spectrum.

The slow subspectrum and the fast subspectrum are rather widely separated (note the logarithmic scale on the ω -axis in Fig. 2).

The frequencies of the eigenoscillations are always below the coronal upper cut-off frequency $\omega \leq \omega_{II}(L_c) = \omega_{II}$. When k_x increases we find that the g -spectrum either ceases to exist or it is shifted into the Alfvén continuum and it becomes impossible to calculate. The p -subspectrum on the other hand exists for any value of k_x . For these reasons we present the results on p -modes and g -modes in two separate subsections. The g -modes for $\beta_p=1.2$ are confined to $0 \leq k_x \leq 0.2 \text{ Mm}^{-1}$ and $0 \leq \text{Re } \omega < 0.02 \text{ rad s}^{-1}$ and the g -modes for $\beta_p=1,000$ are confined to $0 \leq k_x \leq 4 \text{ Mm}^{-1}$ while p -modes exist for all $k_x \geq 0$ and have typically $\text{Re } \omega \approx 1 \text{ rad s}^{-1}$.

6.1. The subspectrum of modified p -modes

Let us now look at results for the high frequency part of the spectrum. For each set of wave numbers k_x and k_y there is a finite number of discrete high frequency modes. The fast subspectrum is computed for $0 \leq k_x \leq 14 \text{ Mm}^{-1}$ and for two values of k_y : $k_y=0$ and $k_y=3.6 \text{ Mm}^{-1}$. For $k_y=0$ the magnetosonic modes are decoupled from the Alfvén modes, for $k_y \neq 0$ they might be coupled to the Alfvén modes and get damped.

For a weak magnetic field ($\beta_p=1,000$), the eigenfrequencies are real in a large domain as can be seen in Fig. 3, where the lower cut-off frequency ω_I is now close to zero. The other characteristic frequencies ω_A and ω_c are much smaller than ω_I and are not shown in the figure. In a strictly nonmagnetic case when $\beta_p \rightarrow \infty$, we have $\omega_A = \omega_c = 0$ and the entire spectrum is real. When k_x is increased we find that the number of modes increases.

For a given set of wave numbers k_x and k_y there is always a finite number of their modes as seen in Fig. 4 where plotted quantities have their dimensional values. The eigenfrequencies are calculated as functions of k_x when $0 \leq k_x \leq 14 \text{ Mm}^{-1}$, for two values of k_y : 0 and 3.6 Mm^{-1} and for $\beta_p=1.2$. As we have seen when the magnetic field was weak, Fig. 4 also shows that the number of existing modes increases with k_x at both values for k_y . The same effect was found when the magnetic field was weaker as seen in Fig. 3 where the eigenfrequencies were plotted for $\beta_p=1,000$. We notice that the number of modes now grows faster with k_x then it does in Fig. 4.

In Fig. 4 we see eigenmodes with complex frequencies as the imaginary part is negative the eigenmodes are damped.

The eigenfrequencies become complex if at least one of the two resonances occurs within the transitional layer i.e. at heights below L_c .

In the case of $k_y=0$, the Alfvén resonance does not exist while the cusp resonance is possible if $\text{Re } \omega < \omega_c = \omega_c(z_L)$. The undamped modes with real frequencies are then those with $\omega > \omega_I > \omega_c$ while the quasimodes have $\text{Re } \omega < \omega_c$ as can be seen in Fig. 4 for $\beta_p=1.2$.

When $k_y \neq 0$, both resonances can appear: the Alfvén resonance alone if $\omega_A > \text{Re } \omega > \omega_c$ or in combination with the cusp resonance if $\text{Re } \omega < \omega_c$. In both cases, we have damped quasimodes with complex frequencies while modes with real frequency exist at frequencies $\omega_{II} > \omega > \omega_A$ in Fig. 4 for $k_y=3.6 \text{ Mm}^{-1}$ and $\beta_p=1.2$.

Fig. 5 shows the eigensolutions for P and ξ_z corresponding to real eigenfrequencies at low values of k_x , as seen in Fig. 4. For $k_x=0.07 \text{ Mm}^{-1}$ and $k_y=3.6 \text{ Mm}^{-1}$ there are only four modes with frequencies 0.235 rad s^{-1} , 0.407 rad s^{-1} , 0.528 rad s^{-1} and 0.621 rad s^{-1} . The eigensolutions for each of these four modes are labeled as p_n with $n=0, 1, 2, 3$ indicating the number of zeros i.e. nodes. The p_0 mode has the lowest eigenfrequency and has no zeros. This mode is a pure surface wave and we consider it also as a modified f -mode. The frequencies of the other modes increase with the number of nodes n which indicates the Sturmian character of the spectrum.

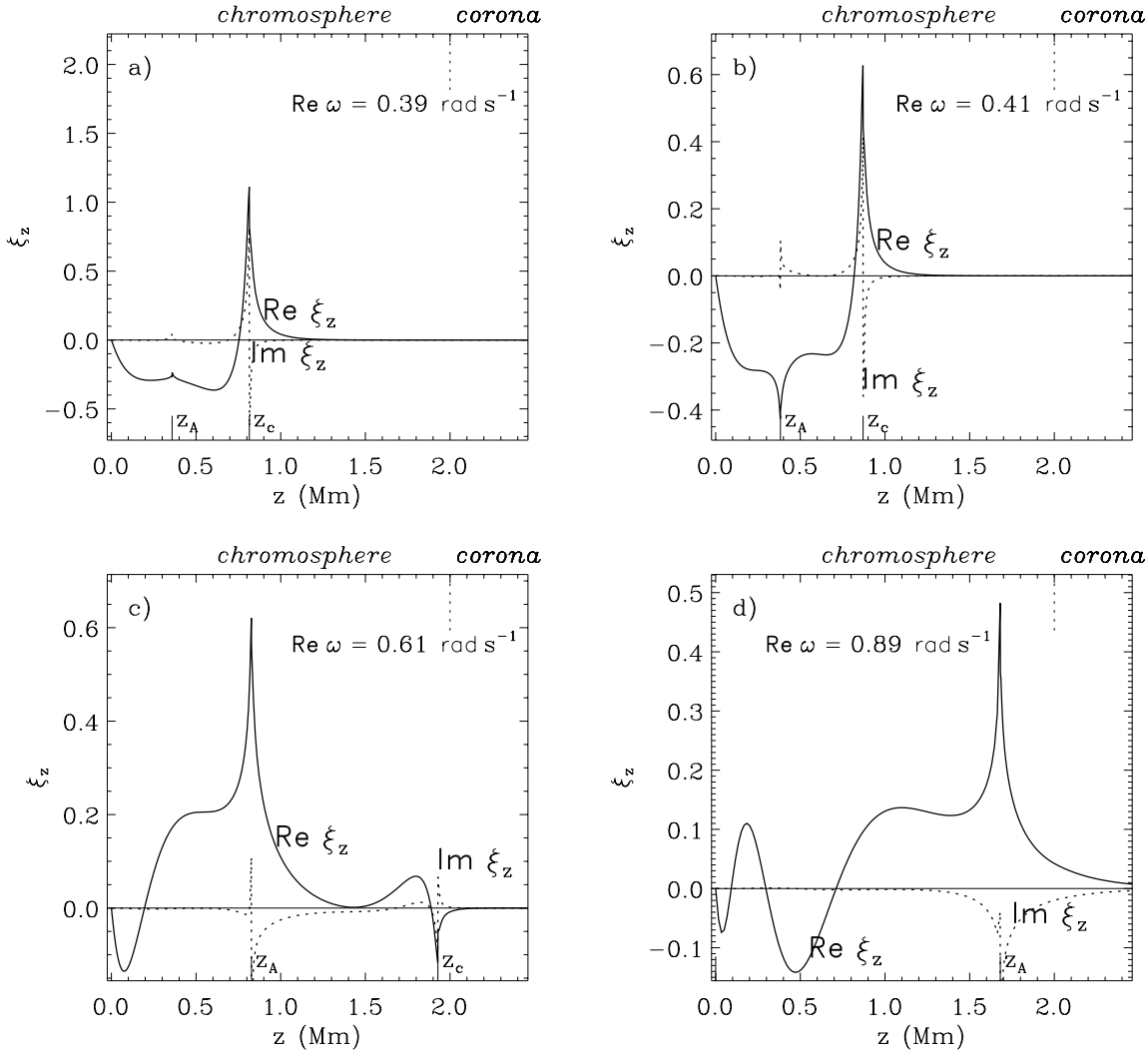


Fig. 6a–d. The eigensolutions $\xi_z(z)$ calculated for $k_x=7.14 \text{ Mm}^{-1}$, $k_y=3.6 \text{ Mm}^{-1}$ and frequencies related to four quasimodes with indicated complex frequencies.

One can also notice from Fig. 5 that the relative values of total pressure perturbation P at maxima exceed those of the displacement ξ_z .

The eigensolutions shown in Fig. 5 also indicate that the modes are spatially trapped inside a cavity bounded by two values of z depending on wave parameters ω , k_x and k_y . The limits of that region are deduced from a condition obtained by local approximation applied to the initial equations (14) when d/dz is replaced by ik_z and when the coefficients in Eqs. (14) are considered approximately constant over the distance $2\pi/k_z$. In this case we have from Eqs. (14):

$$k_z^2(z) = \frac{C_2(z)C_3(z) - C_1^2(z)}{D^2(z)} \quad (32)$$

where the value of k_z depends on z through the coefficients $C_1(z)$, $C_2(z)$, $C_3(z)$ and $D(z)$.

The local condition for propagating waves is now clearly $k_z^2(z) > 0$ with $k_z(z)$ given by (32). The waves are therefore

trapped between the points z that are the solutions of $k_z(z)=0$. As $k_z(z)$ also depends on ω , k_x and k_y , we can calculate the curves $\omega=\omega(z; k_x, k_y)$ where $k_z(z)=0$. These are shown in the upper part of Fig. 9 where they separate the propagating region from the nonpropagating region for $k_x=0.07 \text{ Mm}^{-1}$, $k_y=3.6 \text{ Mm}^{-1}$ and $\beta_p=1.2$.

The effects of resonances on the eigensolution ξ_z are shown in Fig. 6. The eigensolutions $\xi_z(z)$ are calculated for four representative modes with $k_x=7.14 \text{ Mm}^{-1}$ and $k_y=3.6 \text{ Mm}^{-1}$. The frequencies of these four modes are complex with negative imaginary parts meaning that waves are damped. Such waves are called quasimodes and they vanish in a nonmagnetic atmosphere where $\omega_c=0$. Due to this property, we can call them magnetic p -quasimodes. The corresponding real parts of the frequency are $\text{Re } \omega = 0.39 \text{ rad s}^{-1}$, 0.41 rad s^{-1} , 0.61 rad s^{-1} and 0.81 rad s^{-1} (see Fig. 4).

Two of the modes are separated from the remaining part of the p -mode spectrum as seen in Fig. 4 and they appear in pairs

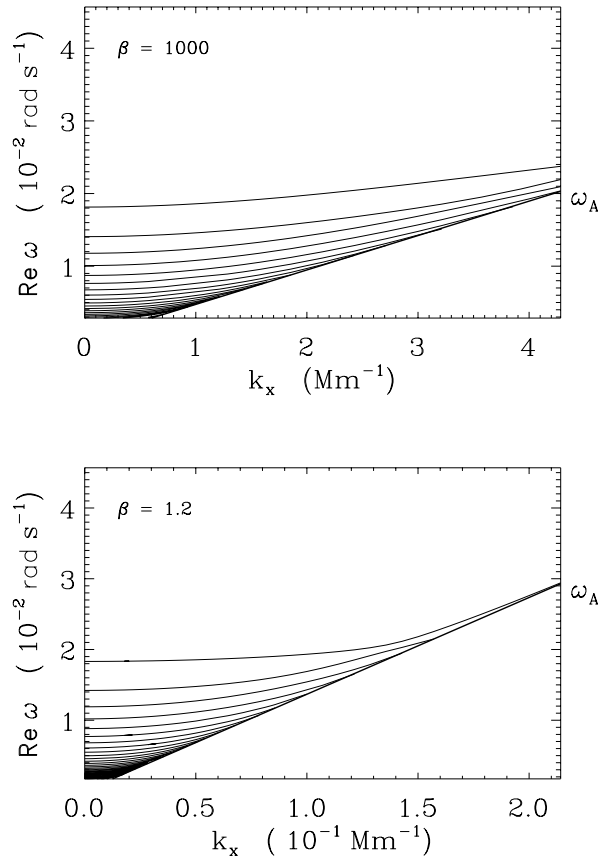


Fig. 7. Modified g -modes for $\beta_p=1,000$ and $\beta_p=1.2$: dispersion curves $\text{Re } \omega(k_x)$ with $k_y=3.6 \text{ Mm}^{-1}$.

with frequencies $\text{Re } \omega = 0.39 \text{ rad s}^{-1}$ and 0.41 rad s^{-1} which are relatively close to each other. These frequencies are smaller than the coronal cusp frequency $\omega_c(L_c)$ so that both the Alfvén and the cusp resonances contribute in wave damping. The complex eigensolutions ξ_z for this pair of modes are displaced in Fig. 6a and Fig. 6b. The plots show peaks with jumps in $\text{Re } \xi_z$ - and in $\text{Im } \xi_z$ -curves at resonant points $z=z_{A,c}$. We see that the effect of the cusp resonance is stronger than the effect of the Alfvén resonance. The latter is almost negligible for the mode with the lower frequency $\omega = 0.39 \text{ rad s}^{-1}$.

The other two modes have complex frequencies, with $\text{Re } \omega = 0.61 \text{ rad s}^{-1}$ and 0.81 rad s^{-1} , and they are magnetic p -quasimodes too. The corresponding eigensolutions ξ_z are shown in Fig. 6c and in Fig. 6d. The solution in Fig. 6c is a damped wave with $\text{Re } \omega < \omega_c < \omega_A$ where both resonances are present. The solution in Fig. 6d refers to a quasimode with $\omega_A > \text{Re } \omega > \omega_c$ where damping occurs from the Alfvén resonance only. The solutions for modes with real frequencies in the interval $\omega_{II} > \omega > \omega_A$, are similar to those shown in Fig. 5.

We see in Fig. 6 that the eigensolutions with $k_x=7.14 \text{ Mm}^{-1}$ are localized in space, similarly to solutions with $k_x=0.07 \text{ Mm}^{-1}$ in Fig. 5.

According to the conditions for existence of quasimodes, we conclude that the quasimodes found here are a phenomenon that

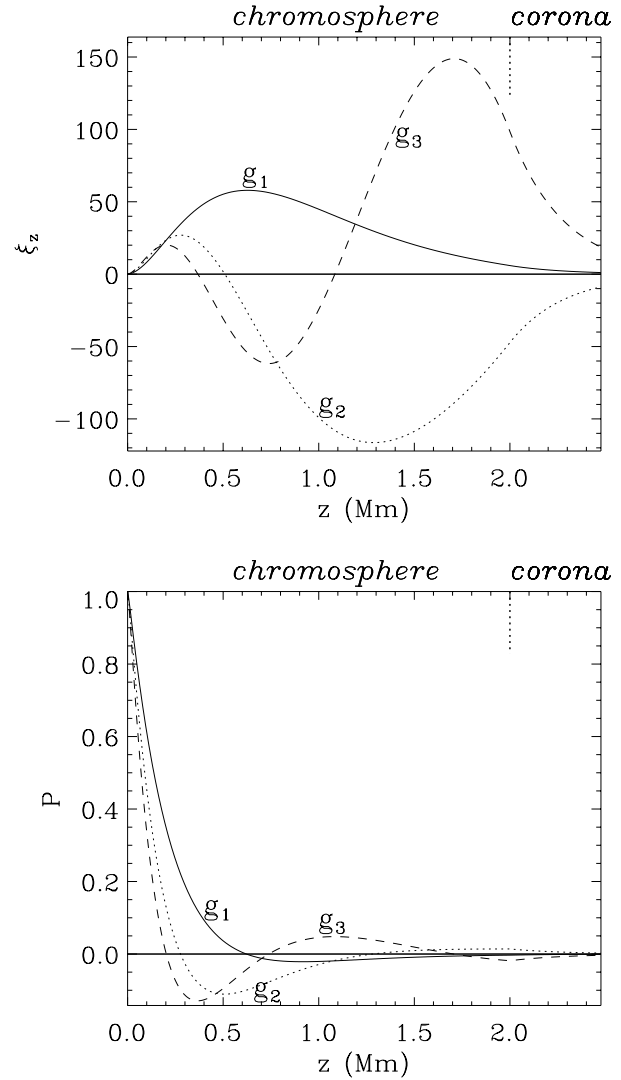


Fig. 8. The eigenvalue solutions for three consecutive modified g -modes with frequencies related to $k_x=0.07 \text{ Mm}^{-1}$ and $k_y=3.6 \text{ Mm}^{-1}$. The number of zeros i.e. nodes, increases when the eigenfrequency is becoming smaller. The spectrum of these waves is therefore anti Sturmian.

requires the presence of a magnetic field. In a nonmagnetic atmosphere $\omega_A=\omega_c=0$ and the p -modes can have real frequencies only.

6.2. The subspectrum of modified g -modes

In addition to the subspectrum of p -modes there is a subspectrum of g -modes.

Fig. 7 shows the spectrum of these modes with real frequencies $\omega(k_x)$ for $\beta_p=1,000$ and $\beta_p=1.2$ and for $k_y=3.6 \text{ Mm}^{-1}$. The frequencies of these modes are bounded from above and from below and are getting spaced more densely as the frequency decreases.

Fig. 8 shows the eigensolutions $\xi_z(z)$ and $P(z)$ for the first three modes, labeled by g_n ($n=1, 2, 3$) with the corresponding

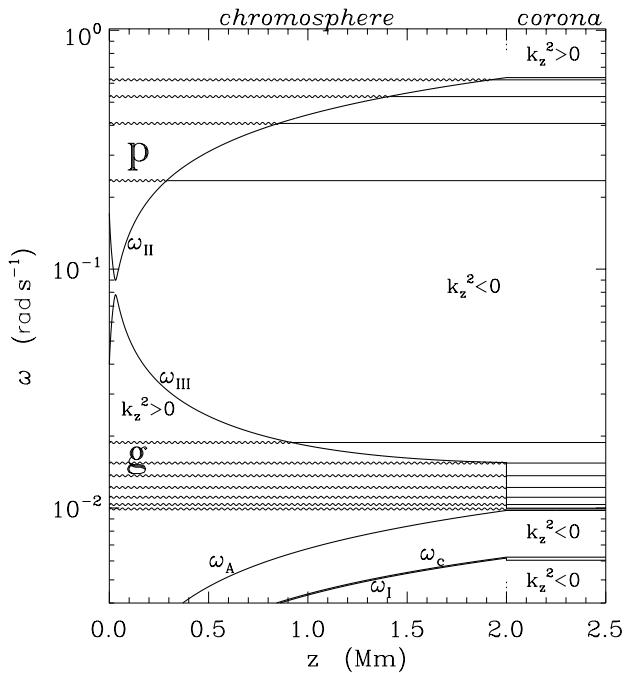


Fig. 9. The cavities for trapped modified p - and g -modes for $k_x=0.07 \text{ Mm}^{-1}$, $k_y=3.6 \text{ Mm}^{-1}$ and $\beta_p=1.2$.

frequencies $\omega_n=1.88 \cdot 10^{-2} \text{ rad s}^{-1}$, $1.54 \cdot 10^{-2} \text{ rad s}^{-1}$ and $1.37 \cdot 10^{-2} \text{ rad s}^{-1}$ related to $k_x=0.07 \text{ Mm}^{-1}$ and $k_y=3.6 \text{ Mm}^{-1}$. The number of nodes increases with n while the frequency of the mode decreases with increasing of n . The spectrum of modified g -modes is therefore anti-Sturmian.

The modified g -modes are trapped in a cavity and a procedure analogous to that described for the modified p -modes yields the frequency dependent trapping regions as shown in Fig. 9.

Comparing the relative values of ξ_z and P in Fig. 8, we see that the total pressure perturbation amplitudes are by several orders of magnitude smaller than those of the displacement ξ_z . This means that the perturbations of the magnetic pressure and of the thermal pressure are mutually compensated in modified g -modes.

7. Conclusions

We have studied the eigenmodes of a stellar atmosphere composed of a chromospheric layer with a linear equilibrium temperature profile, and an isothermal corona above the chromosphere. The atmosphere is permeated by a horizontal magnetic field which is uniform in the chromosphere and of a decreasing strength in the corona where the speed of sound and the Alfvén speed are taken constant. As the plasma of the atmosphere is much thinner than the medium of the stellar interior, we consider the photosphere as a solid and immobile boundary for the atmosphere. The atmosphere is therefore assumed isolated i.e. decoupled from global solar oscillations.

For such a configuration, the solutions show the existence of two distinct subspectra of eigenmodes that are analogous to the known global internal modes of the solar main body: the p - and the g -modes. For this reason, we call the two subspectra of eigenmodes of our model atmosphere the modified p - and the modified g -modes.

We found in our model that the modified p -modes are compressional waves with a Sturmian spectrum while the modified g -modes induce practically no perturbation in the total pressure and have an anti-Sturmian spectrum.

An important consequence of the presence of magnetic field in our model is the appearance of resonant coupling of eigenmodes to the local cusp and to the local Alfvén continuum modes. This results into wave damping and the modes are called quasimodes. As the wave energy is dissipated by its conversion into heat, the quasimodes play a role in the process of atmospheric heating.

As an example, we take numerical values for the basic state parameters that are close to the values in solar conditions. The temperature ratio between the photosphere and the corona is $\tau=200$, the other photospheric values are the temperature $T_p=6,000 \text{ K}$, the plasma beta parameter is $\beta_p=1.2$ and $1,000$ while the thickness of the chromospheric layer is taken $L_c=2 \text{ Mm}$. The oscillation periods for the modified p -modes are not shorter than 0.5 min while the modified g -modes have periods longer than 5 min .

Acknowledgements. V.Čadež acknowledges the financial support by the 'Onderzoeksfonds K.U.Leuven' (senior research fellowships F/95/62 and F/97/9) while B.Pintér thanks the Hungarian Soros Foundation for the financial support.

References

- Evans, P. & Roberts, B., 1990, ApJ 356, 704.
- Goossens, M., Ruderman, M.S. & Hollweg, J.V., 1995a, Solar Physics 157, 75.
- Goossens, M. & Ruderman, M.S., 1995, Physica Scripta T60, 171.
- Jain, R. & Roberts, B., 1993, ApJ 414, 898.
- Jain, R. & Roberts, B., 1994, A&A 286, 243.
- Miles, A.J. & Roberts B., 1992, Solar Physics 141, 205.
- Miles, A.J., Allen, H.R. & Roberts G., 1992, Solar Physics 141, 235.
- Poedts, S. & Kerner, W., 1991, Phys. Rev. Letters 66, 22.
- Ruderman, M.S., Tirry, W. & Goossens, M., 1995, J. Plasma Physics 54, 129.
- Sakurai, T., Goossens, M. & Hollweg, J.V., 1991a, Solar Physics 133, 227.
- Sakurai, T., Goossens, M. & Hollweg, J.V., 1991b, Solar Physics 133, 247.
- Tirry, W.J. & Goossens, M., 1996, ApJ., 471, 501.
- Tirry, W.J., Goossens, M., Pintér, B., Čadež, V.M. & Vanlommel, P., 1997, sent to ApJ.